Zinc(II) complexes with Schiff bases derived from ethylenediamine and salicylaldehyde: the synthesis and photoluminescent properties

O. V. Kotova,[a]★ S. V. Eliseeva,[a] A. S. Averjushkin,[b] L. S. Lepnev,[b] A. A. Vaschenko,[b] A. Yu. Rogachev,[c] A. G. Vitukhnovskii,[b] and N. P. Kuzmina[a]

[a]*Department of Chemistry, M. V. Lomonosov Moscow State University, 1 Leninskie Gory, 119991 Moscow, Russian Federation. Fax: +7 (495) 939 0998. E-mail: kotova@inorg.chem.msu.ru*
[b]*P. N. Lebedev Physical Institute, Russian Academy of Sciences, 53 Leninsky prosp., 119991 Moscow, Russian Federation. Fax: +7 (499) 135 7860. E-mail: alexei@sci.lebedev.ru*
[c]*Department of Chemistry, University at Albany, State University of New York, USA, 12222-0100 New York, Albany. Fax: (518) 442 3462. E-mail: rogachev@albany.edu*

The effect of the nature of organic ligands and complex formation on the photoluminescent characteristics (relative quantum yield, excited-state lifetime) and thermal stability of tetradentate Schiff bases (H_2L), derivatives of salicylaldehyde ($H_2(SAL)^1$, $H_2(SAL)^2$), *o*-vanillin ($H_2(MO)^1$, $H_2(MO)^2$) with ethylenediamine and *o*-phenylenediamine, and their zinc(II) complexes was studied. Zinc(II) complexes were synthesized by the reaction of H_2L with $Zn(AcO)_2 \cdot 2H_2O$ in MeOH at room temperature or under reflux. In the case of $H_2L = H_2(SAL)^2$, $H_2(MO)^1$, $H_2(MO)^2$, complexes of the composition $ZnL \cdot H_2O$ were isolated irrespective of the temperature. For $H_2L = H_2(SAL)^1$, the reaction results in $Zn(SAL)^1 \cdot H_2O$ at room temperature and in anhydrous dimeric complex $[Zn(SAL)^1]_2$ under reflux. Density functional calculations of H_2L and ZnL confirmed that (1) luminescence of these compounds is due to the $\pi—\pi^*$ transition between orbitals of the organic ligand and (2) enhancement of conjugation of the chain and introduction of electron-donating substituents lead to a decrease of the energy gap and, therefore, to a bathochromic shift of the emission maximum.

Key words: Schiff bases, zinc(II) complexes, luminescence, organic light emitting diodes.

Transition metal coordination compounds (CC) exhibiting luminescent properties are of interest because they can be used as electroluminescent (EL) materials for organic light emitting diodes (OLED).[1—5] Determination of correlations between the composition, structure, and functional properties (luminescence, thermal stability, volatility, conductivity, *etc.*) of starting CC underlies the design of new EL materials. Investigations of the effect of substituents in organic ligands on the photophysical properties of complexes have been documented.[6—8] Taking an aluminum(III) complex with 8-oxyquinoline (AlQ_3, λ_{max} = 525 nm) as an example, it was shown that the introduction of electron-donating substituents to the benzene fragment leads to a bathochromic shift of the emission maximum and to a hypsochromic shift if the substituent was introduced into the pyridine fragment. This effect was explained[9] by the change in the band structure. In addition, many researchers pay attention to the effect of introduction of conjugated benzene rings into CC. $\pi—\pi$ Interaction between them causes a bathochromic shift of the emission maximum[10,11] and a decrease in the quantum yield of photoluminescence,[12] as well as an increase in conductivity.[13] However, in each case the study of the effect of the nature of organic ligands on the composition and functional properties of the CC based on them is a subject of separate investigation.

Among different classes of zinc(II) CC, which are of interest as the EL materials, complexes with organic ligands containing the azomethine C=N bond and a donor oxygen or nitrogen atom are of special interest because these systems exhibit intense luminescence in the blue region of the visible spectrum.[1,4,14—16] Interest in the search for new sources of blue luminescence is due to the fact that efficient EL materials, *i.e.*, red and green luminophores, are already found among CC and used in OLED, whereas blue luminophores of comparable efficiency have not been found so far.[3—5] Luminescent properties of zinc(II) complexes are determined only by the organic ligand because the d-shell of the central ion is completely filled. In addition, the nature of organic ligands in CC considerably in-

Published in Russian in *Izvestiya Akademii Nauk. Seriya Khimicheskaya,* No. 9, pp. 1846—1855, September, 2008.
1066-5285/08/5709-1880

fluences the packing of molecules in the crystal structure and the formation of intermolecular contacts,[17,18] which also affect the luminescent properties. This enables targeted variation of the functional properties of zinc(II) CC by the introducing different substituents into organic ligands.

In the present work, we study the effect of conjugation enhancement by replacement of the ethylenediamine bridge with the *o*-phenylenediamine one (in the pairs $H_2(SAL)^1$—$H_2(SAL)^2$, $H_2(MO)^1$—$H_2(MO)^2$) and by introduction of electron-donating substituents (in particular, methoxy group at position 1,1′ in the pairs $H_2(SAL)^1$—$H_2(MO)^1$, $H_2(SAL)^2$—$H_2(MO)^2$) on the photoluminescent and thermal properties of Schiff bases (H_2L) and zinc(II) complexes ($ZnL \cdot H_2O$).

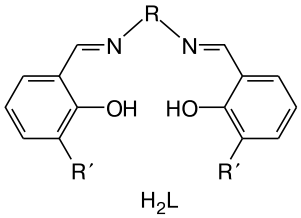

H_2L

R	R′	L
—CH_2—CH_2—	H	$(SAL)^1$
	H	$(SAL)^2$
—CH_2—CH_2—	OMe	$(MO)^1$
	OMe	$(MO)^2$

The influence of the ligand nature on the topology of the frontier orbitals and their position on the energy scale was evaluated and theoretical modeling of the systems H_2L and ZnL in the framework of the DFT approach was performed.

Experimental

Starting compounds $Zn(AcO)_2 \cdot 2H_2O$ (chemically pure grade), ethylenediamine (chemically pure grade), *o*-phenylenediamine (chemically pure grade), *o*-vanillin (Aldrich), methanol (Aldrich), benzene (chemically pure grade) were used without additional purification. Salicylaldehyde (pure grade) was purified by distillation *in vacuo* (b.p. 93 °C, 25 Torr).

Synthesis of Schiff bases was carried out according to a standard procedure[19] by the reaction of an aldehyde ($2 \cdot 10^{-3}$ mol) and the corresponding diamine ($1 \cdot 10^{-3}$ mol) in benzene. The yields were ~90—95%.

Synthesis of zinc(II) complexes.[20,21] Reactions of solutions of zinc(II) acetate ($1 \cdot 10^{-3}$ mol) and a Schiff base ($1 \cdot 10^{-3}$ mol) in MeOH at room temperature and under reflux led to precipitation of corresponding zinc(II) complexes. For more complete precipitation, the reaction mixtures were cooled to 5 °C. The precipitates were isolated by filtration. The yields were ~70%.

The percentage of carbon, hydrogen, and nitrogen was determined by elemental microanalysis on a C,H,N-analyzer at the Center for Pharmaceutical Chemistry of the All-Russian Chemical and Pharmaceutical Research Institute (CPC-ARCPRI).

IR spectra of the complexes were recorded on a Perkin—Elmer FT-IR-1600 spectrometer in the region 4000—400 cm^{-1} (samples were suspended in Nujol and hexachlorobutadiene).

^1H NMR spectra were recorded on a Bruker Avance-400 spectrometer (400 MHz).

Mass spectra (EI) of zinc(II) complexes were recorded on a SSQ-710 instrument (Finigan MAT, USA) at CPC-ARCPRI.

X-Ray phase analysis of powdered complexes was performed on a STADI/IP diffractometer (Cu-Kα irradiation). Calculations of theoretical X-ray patterns, as well as indexing were performed using the STOE WinXPOW 1.04 program package.*

Thermal analysis was carried out on a Q-1500 derivatograph in the temperature range 20—700 °C under nitrogen atmosphere (sample weight 0.05—0.1 g, heating rate ~10 °C min^{-1}).

Photoluminescence spectra of solid samples of the Schiff bases and zinc(II) complexes were measured on an Ocean Optics S2000 multichannel spectrometer (an LGI-21 nitrogen laser as the source of photoexcitation; λ_{exc} = 337 nm) at 25 °C and at the temperature of liquid nitrogen (−196 °C). A correction for the instrument function was made for all the photoluminescence spectra. The relative quantum yield of photoluminescence (φ_{rel}) was calculated according to Ref. 22. The accuracy in the determination of φ_{rel} was ±10%.

Excited-state lifetimes (τ_{obs}) were measured on a Model 199s fluorescent spectrometer (Edinburgh Instruments Ltd.) using a nitrogen gas-discharge lamp (λ_{exc} = 337 nm, τ = 3 ns) and averaged at least over three independent measurements. The luminescence decay curves were recorded at a wavelength corresponding to the maximum intensity of the sample photoluminescence. To calculate the luminescence decay times for the samples under study, the experimental decay curves were deconvoluted with allowance for the decay time of the nitrogen gas-discharge lamp. All the decay curves were fitted by monoexponential functions.

Theoretical modeling was accomplished in the framework of the DFT approach using the B3LYP exchange-correlation potential[23]. Zinc(II) ions were described using the Hay—Wadt effective core potential and the basis set LANL2DZ.[24] For the atoms of organic ligands, the standard split-valence basis sets 6-311G augmented with polarization d-functions for the non-hydrogen atoms and p-functions for the hydrogen atoms (6-311G(d,p)) were used. Full geometry optimization of enol—enol tautomers of the Schiff bases and zinc complexes corresponding to the minima on the potential energy surface (PES) was conducted until a gradient of 10^{-5} at.u. assuming the point symmetry group C_2. In the case of enol—keto forms of organic molecules, no symmetry restrictions were imposed (point symmetry group C_1). The spin multiplicities of the Schiff bases and zinc(II) complexes were set equal to 1. The absence of calculated imaginary harmonic vibrational frequencies suggests that the optimized structures correspond to the energy minima on the corresponding PES. All calculations were carried out using the PC GAMESS program package.** Despite the fact that theoretical

* http://www.stoe.com

** A. A. Granovsky, URL http://lcc.chem.msu.ru/gran/gamess/index.html

modeling was performed in the isolated molecule approximation ignoring the effect of the aggregation state or solvent, the qualitative estimation of changes in the series of same-type compounds is justified, as well as the analysis of the nature of transitions. For visualization (isosurfaces with an increment of 0.035 a.u.) and analysis of the molecular orbitals (MO) of the systems under study, the ChemCraft program* was used.

***N*,*N*′-Ethylene-bis(salicylidenediamine) $H_2(SAL)^1$.** Found (%): C, 71.4; H, 5.9; N, 10.4. $C_{16}H_{16}N_2O_2$. Calculated (%): C, 71.6; H, 5.9; N, 10.5. IR, ν/cm^{-1}: 3052, 3010, 2956, 2930, 2900, 2870 (ν(C—H) + (N—H)); 1636 (ν(C=N)); 1577, 858, 775, 742, 648, 562, 473 (Ar ring vibrations); 1372, 1284 (δ(O—H)); 1200, 1150, 1042, 1021 (ν(C—O)). ^{1}H NMR ($CDCl_3$/Me_4Si), δ: 13.20 (s, 2 H); 8.33, 7.29, 7.21, 6.93, 6.84 (all s, 2 H each); 3.90 (s, 4 H).

***N*,*N*′-(*o*-Phenylene)-bis(salicylidenediamine) $H_2(SAL)^2$.** Found (%): C, 75.7; H, 5.1; N, 9.0. $C_{20}H_{16}N_2O_2$. Calculated (%): C, 75.9; H, 5.1; N, 8.9. IR, ν/cm^{-1}: 3053, 2988, 2927, 2855, 2712 (ν(C—H) + ν(N—H)); 1612 (ν(C=N)); 1562, 831, 761, 640, 581, 512 (Ar ring vibrations); 1362, 1277 (δ(O—H)); 1192, 1150, 1044, 1028 (ν(C—O)). ^{1}H NMR ($CDCl_3$/Me_4Si), δ: 13.05, 8.59, 7.34, 7.33, 7.30, 7.19, 7.03, 6.89 (all s, 2 H each).

***N*,*N*′-Ethylene-bis(3-methoxysalicylidenediamine) $H_2(MO)^1$.** Found (%): C, 65.6; H, 6.3; N, 8.6. $C_{18}H_{20}N_2O_4$. Calculated (%): C, 65.9; H, 6.1; N, 8.5. IR, ν/cm^{-1}: 3087, 3006, 2932, 2915, 2841, 2585 (ν(C—H) + ν(N—H)); 1633 (ν(C=N)); 837, 792, 731, 621 (Ar ring vibrations); 1324, 1250, 1081, 1048, 1010 (δ(O—H)); 1190, 1170, 1132 (ν(C—O)). ^{1}H NMR ($CDCl_3$/Me_4Si), δ: 13.59, 8.33, 6.91, 6.85, 6.79 (all s, 2 H each); 3.96 (s, 4 H); 3.89 (s, 6 H).

***N*,*N*′-(*o*-Phenylene)-bis(3-methoxysalicylidenediamine) $H_2(MO)^2$.** Found (%): C, 69.7; H, 5.8; N, 8.2. $C_{22}H_{20}N_2O_4$. Calculated (%): C, 70.2; H, 5.3; N, 7.5. IR, ν/cm^{-1}: 3464, 3369, 3058, 3014, 2955, 2925, 2837 (ν(C—H) + ν(N—H)); 1613 (ν(C=N)); 736, 648, 584, 539 (Ar ring vibrations); 1400, 1378, 1366, 1324, 1246 (δ(O—H)); 1205, 1094, 1040 (ν(C—O)). ^{1}H NMR ($CDCl_3$/Me_4Si), δ: 13.20, 8.62, 7.34, 7.23, 7.11, 7.02, 6.88 (all s, 2 H each); 3.91 (d, 6 H).

Zinc(II) [*N*,*N*′-ethylene-bis(salicylidenediamine)] monohydrate $Zn(SAL)^1 \cdot H_2O$. Found (%): C, 54.8; H, 4.7; N, 8.1. $C_{16}H_{16}N_2O_3Zn$. Calculated (%): C, 54.9; H, 4.6; N, 8.0. IR, ν/cm^{-1}: 3046, 3018, 2950, 2922, 2930, 2900, 2870 (ν(C—H)); 1654, 1634 (ν(C=N) + δ(O—H)$_{H2O}$); 1596, 1550, 1530, 1514, 860, 850, 744, 740, 634, 608, 572 (Ar ring vibrations); 1184, 1142, 1124, 1090 (ν(C—O)); 3300—2900 (ν(O—H)$_{H2O}$). MS, *m*/*z*: 330 $[Zn(SAL)^1 - H^+]^+$.

Zinc(II) [bis-(*N*,*N*′-ethylene-bis(salicylidenediamine)] $[Zn(SAL)^1]_2$. Found (%): C, 58.5; H, 4.7; N, 8.5. $C_{32}H_{28}N_4O_4Zn_2$. Calculated (%): C, 57.9; H, 4.2; N, 8.5. IR, ν/cm^{-1}: 2898, 2846 (ν(C—H)); 1530, 1540 (ν(C=N)); 1436, 946, 860, 734 (Ar ring vibrations); 1184, 1130, 1125, 1090 (ν(C—O)). MS, *m*/*z*: 330 $[Zn(SAL)^1 - H^+]^+$.

Zinc(II) [*N*,*N*′-(*o*-phenylene)-bis(salicylidenediamine)] monohydrate $Zn(SAL)^2 \cdot H_2O$. Found (%): C, 60.2; H, 4.2; N, 7.1. $C_{20}H_{16}N_2O_3Zn$. Calculated (%): C, 60.5; H, 4.0; N, 7.1. IR, ν/cm^{-1}: 2920, 2820, 2898 (ν(C—H)); 1614 (ν(C=N) + δ(O—H)$_{H_2O}$); 1586, 1530, 854, 800, 748, 602, 552 (Ar ring vibrations); 1170, 1152, 1126, 1034 (ν(C—O)); 3400—2800 (ν(O—H)$_{H_2O}$). MS, *m*/*z*: 378 $[Zn(SAL)^2 - H^+]^+$.

* http://www.chemcraftprog.com

Zinc(II) [*N*,*N*′-ethylene-bis(3-methoxysalicylidenediamine)] monohydrate $Zn(MO)^1 \cdot H_2O$. Found (%): C, 52.5; H, 5.0; N, 6.8. $C_{18}H_{20}N_2O_5Zn$. Calculated (%): C, 52.8; H, 4.9; N, 6.9. IR, ν/cm^{-1}: 3056, 3010, 2948, 2896, 2828 (ν(C—H)); 1660, 1644 (ν(C=N) + δ(O—H)$_{H2O}$); 1600, 1546, 856, 726, 638, 584, 552 (Ar ring vibrations); 1170, 1102, 1070, 1044 (ν(C—O)); 3400—3000 (ν(O—H)$_{H2O}$). MS, *m*/*z*: 390 $[Zn(MO)^1 - H^+]^+$.

Zinc(II) [*N*,*N*′-(*o*-phenylene)-bis(3-methoxysalicylidenediamine)] monohydrate $Zn(MO)^2 \cdot H_2O$. Found (%): C, 57.5; H, 4.6; N, 6.2. $C_{22}H_{20}N_2O_5Zn$. Calculated (%): C, 57.8; H, 4.4; N, 6.1. IR, ν/cm^{-1}: 3046, 2924, 2810 (ν(C—H)); 1690, 1614 (ν(C=N) + δ(O—H)$_{H2O}$); 1586, 1540, 862, 788, 738, 584, 560 (Ar ring vibrations); 1192, 1106, 1074, 1048 (ν(C—O)); 3600—3000 (ν(O—H)$_{H_2O}$). MS, *m*/*z*: 438 $[Zn(MO)^2 - H^+]^+$.

Results and Discussion

Synthesis and characterization. The Schiff bases H_2L = $H_2(SAL)^1$, $H_2(SAL)^2$, $H_2(MO)^1$, and $H_2(MO)^2$ studied in the present work were obtained following standard procedures[19] in high yields (~90%). The composition H_2L was confirmed by elemental analysis, IR spectroscopy, and ^{1}H NMR spectroscopy. The IR spectra exhibit the characteristic bands of the ν(C=N) (in the region 1640—1610 cm^{-1}), ν(O—H) (1400—1000 cm^{-1}), aromatic ring, ν(C—H) and ν(N—H) (3100—2500 cm^{-1}) vibrations. The appearance of the ν(N—H) absorption bands in the IR spectra and the presence of singlet signals at δ ~8.33—8.62 in the ^{1}H NMR spectra confirm the formation of hydrogen bonds O—H...N=C between the hydroxyl hydrogen and the nitrogen atom.[25,26]

Zinc(II) complexes were obtained by reactions of zinc(II) acetate solution with corresponding Schiff base in methanol at room temperature or on heating:

$$Zn(AcO)_2 \cdot 2H_2O + H_2L \rightarrow ZnL \cdot nH_2O. \qquad (1)$$

In the case of H_2L = $H_2(SAL)^2$, $H_2(MO)^1$, and $H_2(MO)^2$, the composition of the products of reaction (1) is independent of temperature and the $ZnL \cdot H_2O$ complexes are isolated. For H_2L = $H_2(SAL)^1$, reaction (1) at room temperature results in $Zn(SAL)^1 \cdot H_2O$, whereas an anhydrous complex $[Zn(SAL)^1]_2$ is formed under reflux. The IR spectra of the zinc complexes exhibit the characteristic absorption bands of the ν(C—H), ν(C=N), ν(C—O) stretching vibrations, and the aromatic ring vibrations. The presence of water molecules in the compounds $ZnL \cdot H_2O$ is indicated by a broad O—H stretching absorption band in the region 3500—3200 cm^{-1}, which is absent in the IR spectrum of $[Zn(SAL)^1]_2$. The X-ray data for $Zn(SAL)^1 \cdot H_2O$ and $[Zn(SAL)^1]_2$ were reported earlier.[27,28] For the products formed in the reaction of zinc(II) acetate with $H(SAL)^1$, a comparison was made of the theoretical diffraction patterns calculated from the data of X-ray analysis for $Zn(SAL)^1 \cdot H_2O$ and $[Zn(SAL)^1]_2$ with

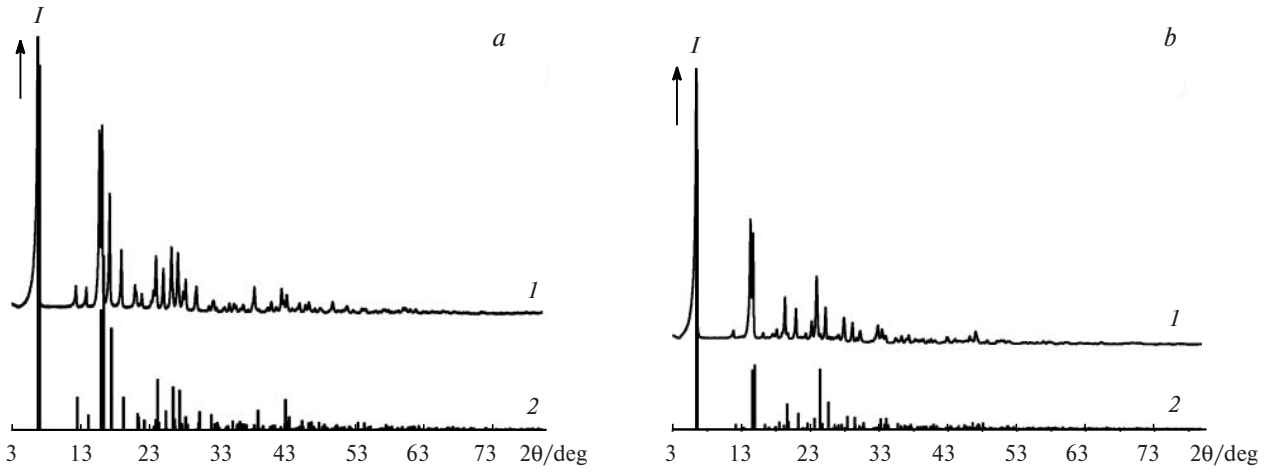

Fig. 1. Experimental (*1*) and theoretically calculated (*2*) X-ray diffraction patterns of $Zn(SAL)^1 \cdot H_2O$ (*a*) and $[Zn(SAL)^1]_2$ (*b*).

the experimental diffraction patterns of the complexes isolated (Fig. 1). For instance, the diffraction pattern of the product of the room-temperature reaction (1) matches the theoretically calculated pattern for $Zn(SAL)^1 \cdot H_2O$, whereas the diffraction pattern of the compound obtained under reflux matches that calculated for the dimer complex $[Zn(SAL)^1]_2$.

Thermal analysis. Thermal stability is an important characteristic of the compounds to be used as the EL materials.[2,3,29] Usually, it is experimentally determined from the weight loss curves. The thermal stability is often characterized by the temperature of the onset of weight loss. Thermal analysis was carried out for the Schiff bases and zinc(II) complexes (Fig. 2). The weight loss curves of H_2L have two portions, the total weight loss is 100%, and the temperatures of the onset of weight loss decrease in the order $H_2(MO)^2$ (250 °C) > $H_2(MO)^1$ (210 °C) > $H_2(SAL)^2$ (160 °C) > $H_2(SAL)^1$ (100 °C).

For $ZnL \cdot H_2O$ (see Fig. 2) in the temperature range 20—150 °C, is characterized by slow weight loss corresponding to elimination of water molecules. The temperature, at which the second stage of weight loss begins, decreases in the order $Zn(SAL)^1 \cdot H_2O$ (320 °C) > $Zn(SAL)^2 \cdot H_2O$ (290 °C) > $Zn(MO)^2 \cdot H_2O$ (230 °C) ≅ $Zn(MO)^1 \cdot H_2O$ (225 °C). For $[Zn(SAL)^1]_2$, the stage of slow weight loss is absent and transformations begin at ~320 °C.

Photoluminescent properties. All the Schiff bases and zinc(II) complexes based on them studied in the present work emit in the visible region on the UV excitation (Fig. 3). The position of emission maximum, the quantum yield of luminescence, and the excited-state lifetime depend on the structure of CC and the nature of the organic ligand. The photoluminescence spectra of H_2L and zinc(II) complexes recorded at the temperature of liquid nitrogen exhibit a hypsochromic shift and a splitting of the emission

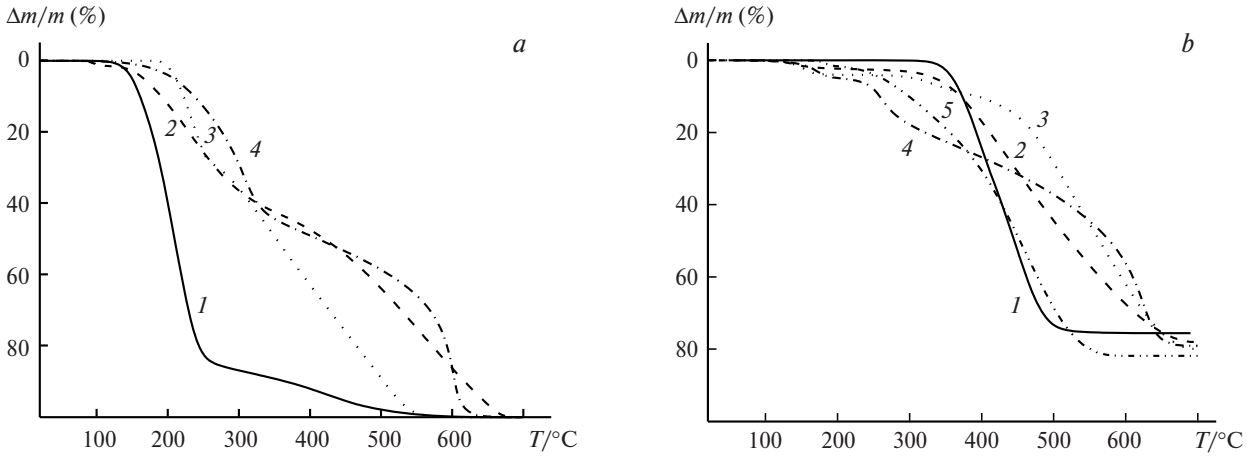

Fig. 2. Weight loss curves of the Schiff bases (*a*) and zinc(II) complexes (*b*) under nitrogen atmosphere: *a*: $H_2(SAL)^1$ (*1*), $H_2(SAL)^2$ (*2*), $H_2(MO)^1$ (*3*), and $H_2(MO)^2$ (*4*); *b*: $[Zn(SAL)^1]_2$ (*1*), $Zn(SAL)^1 \cdot H_2O$ (*2*), $Zn(SAL)^2 \cdot H_2O$ (*3*), $Zn(MO)^1$ (*4*), and $Zn(MO)^2$ (*5*).

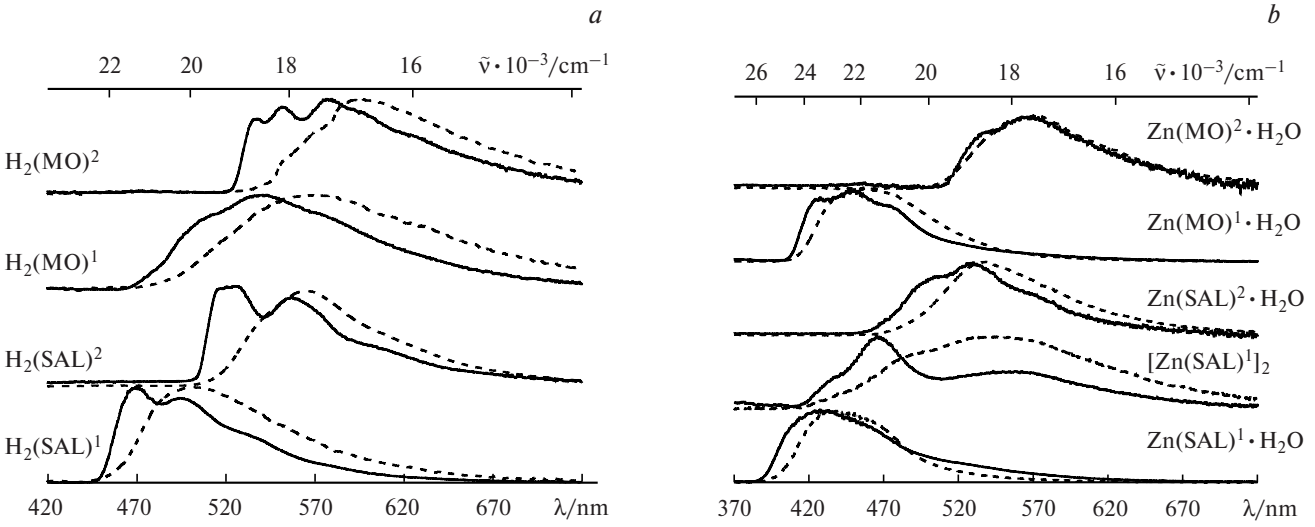

Fig. 3. Photoluminescence spectra of the Schiff bases (*a*) and the zinc(II) complexes (*b*) at −196 (solid lines) and 25 °C (dashed lines); solid samples; λ_{exc} = 337 nm.

band into several components compared to the spectra recorded at 25 °C (see Fig. 3).

The results of theoretical modeling and analysis of the molecular orbitals (Figs 4 and 5) and the published[30,31] data showed that the broad band in the photoluminescence spectra of the Schiff bases is due to the energy transfer between the highest occupied (HOMO) and the lowest unoccupied (LUMO) MO, the HOMO and LUMO mainly being π-bonding and π*-antibonding in character, respectively. Therefore, this band can be assigned to the π→π*-transition. In addition, photoinduced proton transfer is characteristic of excited Schiff base molecules.[32—38] The absorption of a light quantum results in transfer of a proton in the enol—enol structure of the starting Schiff base (Scheme 1, **A**) to form the enol—keto tautomer (see Scheme 1, **B**). The HOMO of the Schiff base in the enol—keto form (**B**) is mainly localized on the fragment containing the NH group (see Fig. 4). On going from the form **A** to **B** (see Scheme 1), the HOMO is split into two orbitals with close energies, which are localized on different fragments (enol and ketone) takes place; this leads to narrowing of the energy gap between the HOMO and LUMO (Fig. 6). Photoluminescence of the zinc(II) complexes is also due to energy transfer between the HOMO and LUMO of the deprotonated ligands with the HOMO mainly being π-bonding in character and the LUMO mainly being π*-antibonding in character. To sum up, the luminescence is caused by the π→π*-transition between the ligand orbitals (ligand-to-ligand charge transfer).

Analysis of published data[8,30,31,39—41] showed that both conjugation enhancement and the introduction of electron-donating substituents should lead to a considerable decrease in the energy difference between the HOMO and LUMO. This is confirmed by the results of theoretical modeling with evaluation of the frontier orbital energies (see Fig. 6), *viz.*, a replacement of the ethylenediamine bridge by the *o*-phenylenediamine one in the pairs $H_2(SAL)^1$—$H_2(SAL)^2$, and $H_2(MO)^1$—$H_2(MO)^2$, as well as introduction of the electron-donating methoxy groups in the pairs $H_2(SAL)^1$—$H_2(MO)^1$, and $H_2(SAL)^2$—$H_2(MO)^2$. A similar decrease in the energy difference between the frontier orbitals under the action of these two factors can be also observed for the zinc(II) complexes (Fig. 7) becausee their energy band structures are mainly determined by the organic ligands. The theoretically calculated changes in positions of the HOMO and LUMO on conjugation enhancement and introduction of electron-donating groups agrees with the experimental data, namely, the photoluminescence spectra of H_2L and $ZnL\cdot H_2O$ exhibit a bathochromic shift of the emission band maximum (see Fig. 3, Table 1).

It is known that deprotonation of organic ligands and complexation with d^{10}-metals also considerably decrease

Scheme 1

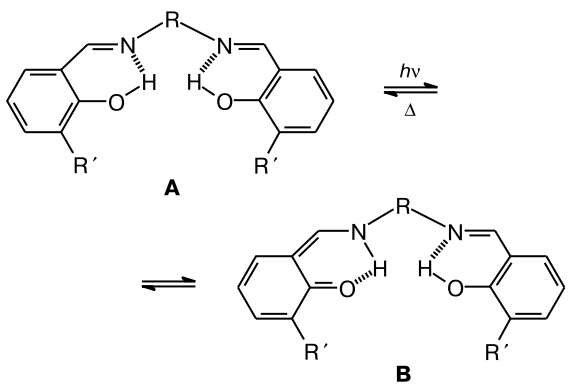

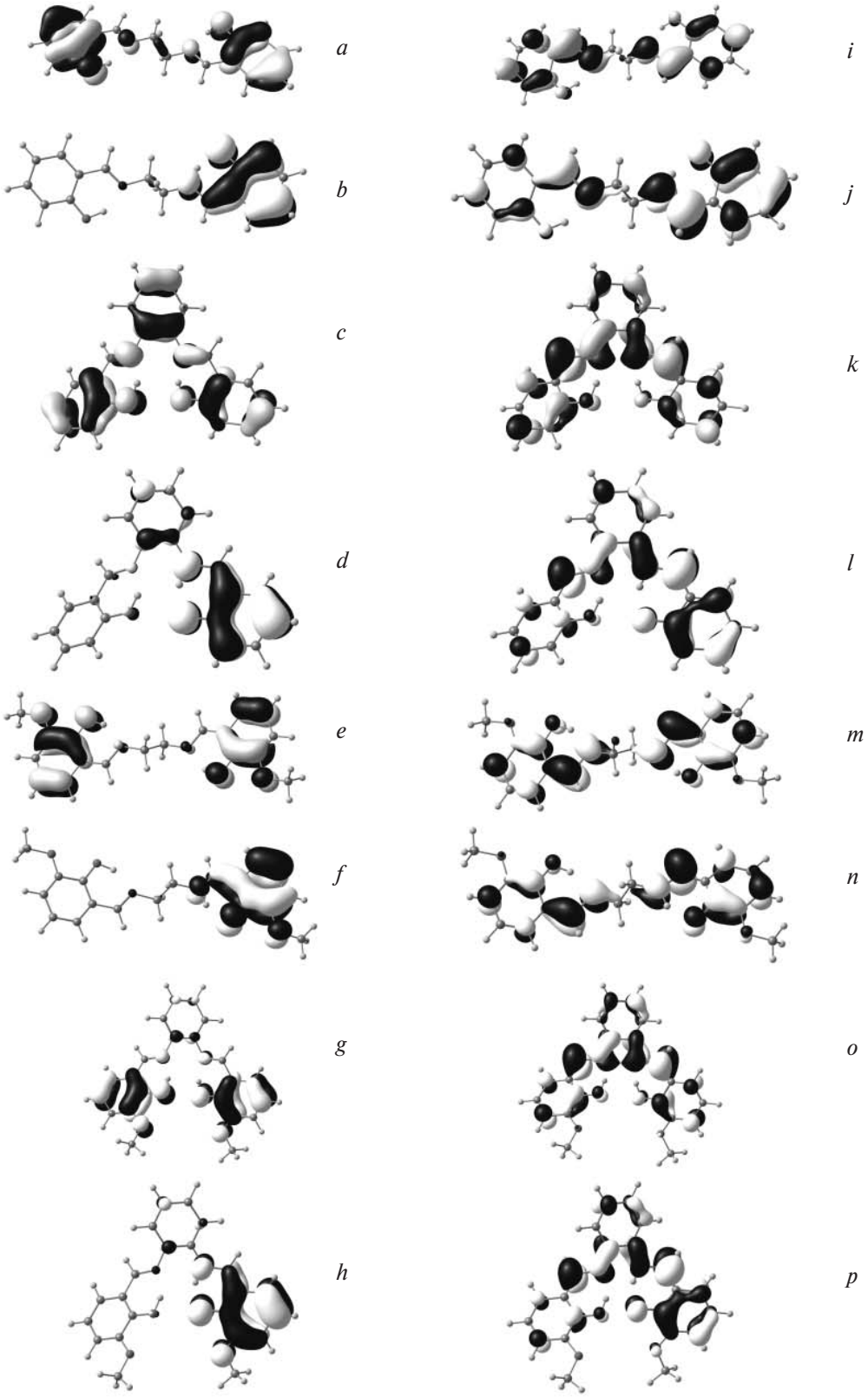

Fig. 4. The highest occupied (*a*—*h*) and lowest unoccupied (*i*—*p*) molecular orbitals of the Schiff bases $H_2(SAL)^1$ (*a*, *b*, *i*, *j*), $H_2(SAL)^2$ (c, *d*, *k*, *l*), $H_2(MO)^1$ (*e*, *f*, *m*, *n*), $H_2(MO)^2$ (*g*, *h*, *o*, *p*) in the enol—enol tautomeric forms (*a*, *c*, *e*, *g*, *i*, *k*, *m*, *o*) and in the enol—keto forms (*b*, *d*, *f*, *h*, *j*, *l*, *n*, *p*) (obtained from B3LYP/6-311G(d,p) calculations).

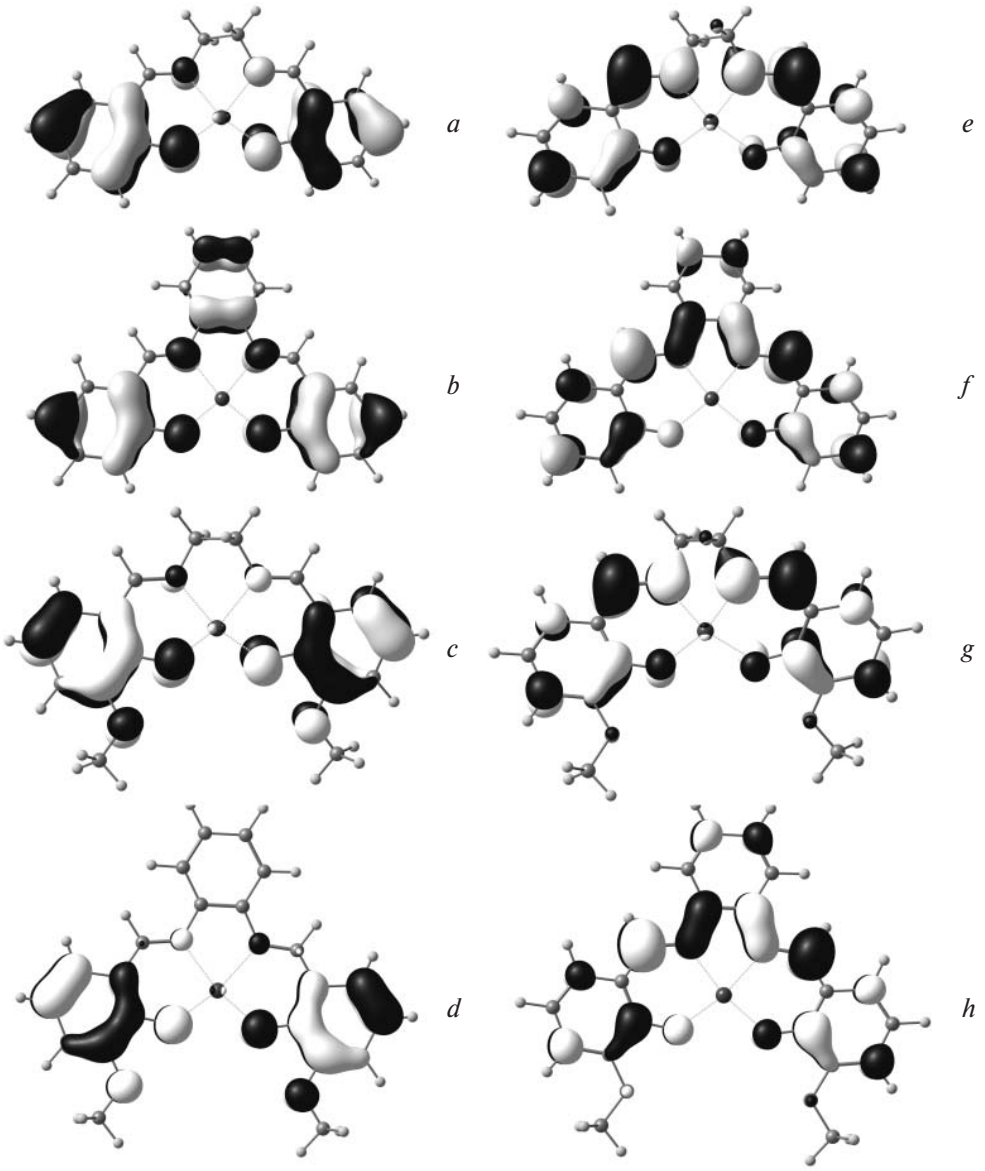

Fig. 5. The highest occupied (*a*—*d*) and lowest unoccupied (*e*—*h*) molecular orbitals of the zinc(II) complexes with Schiff bases $Zn(SAL)^1$ (*a*, *e*), $Zn(SAL)^2$ (*b*, *f*), $Zn(MO)^1$ (c, *g*), and $Zn(MO)^2$ (*d*, *h*) (obtained from B3LYP/LANL2DZ/6-311G(d,p) calculations).

Table 1. Photoluminescence characteristics of the Schiff bases and zinc(II) complexes

Compound	λ_{max}/nm	φ_{rel}/rel. units	τ_{obs}/ns
$H_2(SAL)^1$	501	0.04	0.9
$H_2(SAL)^2$	564	1.00	2.2
$H_2(MO)^1$	571	0.01	0.4
$H_2(MO)^2$	597	0.06	0.7
$Zn(SAL)^1 \cdot H_2O$	436	0.69	2.0
$[Zn(SAL)^1]_2$	540	0.11	1.5
$Zn(SAL)^2 \cdot H_2O$	538	0.10	0.1
$Zn(MO)^1 \cdot H_2O$	457	0.21	1.2
$Zn(MO)^2 \cdot H_2O$	570	0.03	0.2

the energy gap between the HOMO and LUMO. The results of theoretical modeling and comparison of the frontier orbital energies of the Schiff bases in the initial enol—enol form (**A**), and the zinc(II) complexes confirm this regularity (see Fig. 6 and 7). Therefore, the photoluminescence spectra of the zinc(II) complexes should exhibit a bathochromic shift of the emission maximum relative to the spectra of the starting ligands. However, analysis of the experimental data revealed the opposite effect (see Table 1, Fig. 3). Analogous violations of regularities have been documented[42,43] and explained by the intramolecular proton transfer in the excited molecule of the starting Schiff base (Fig. 8). This leads to the bathochromic shift of the H_2L photoluminescence maximum. Complex-

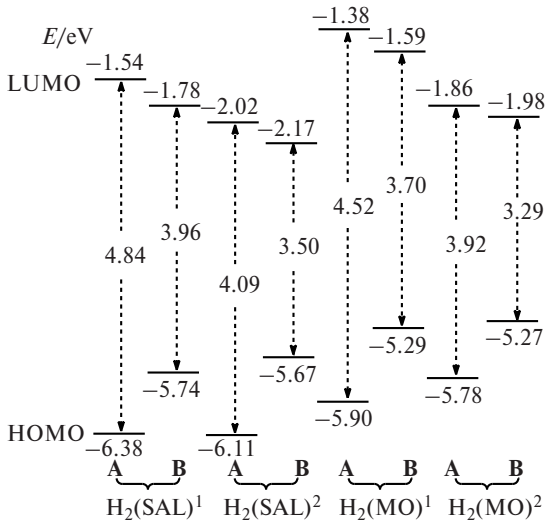

Fig. 6. Theoretical frontier orbital diagrams of tautomeric forms **A** and **B** of the Schiff bases.

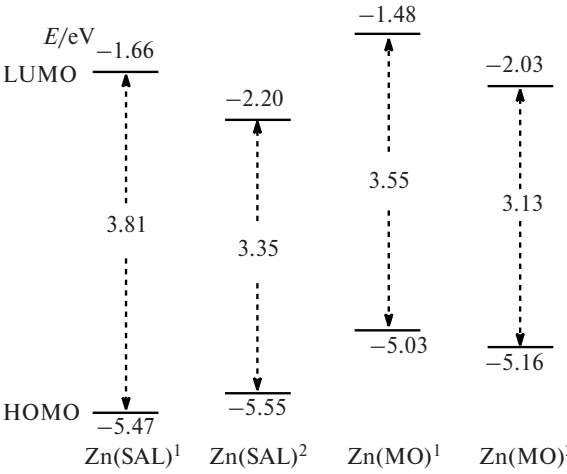

Fig. 7. Theoretical frontier orbital diagrams of the zinc(II) complexes.

ation is accompanied by transformations of these tautomeric forms and, as a consequence, by a hypsochromic shift of the emission maximum in the photoluminescence spectra of the zinc(II) complexes compared to the starting Schiff bases.

Taking the zinc(II) complexes with $H_2(SAL)^1$ as an example, one can determine how their composition and structure affect the photoluminescent properties. For instance, the formation of the dimeric complex $[Zn(SAL)^1]_2$ causes a bathochromic shift of the emission maximum compared to $Zn(SAL)^1 \cdot H_2O$ and the starting $H_2(SAL)^1$ (see Table 1, Fig. 3). The change in positions of the emission maxima of $Zn(SAL)^1 \cdot H_2O$ and $[Zn(SAL)^1]_2$ is explained by different electronic structures of these compounds due to the differences in the crystal structures.[27,28] In both complexes, the coordination polyhedron of the

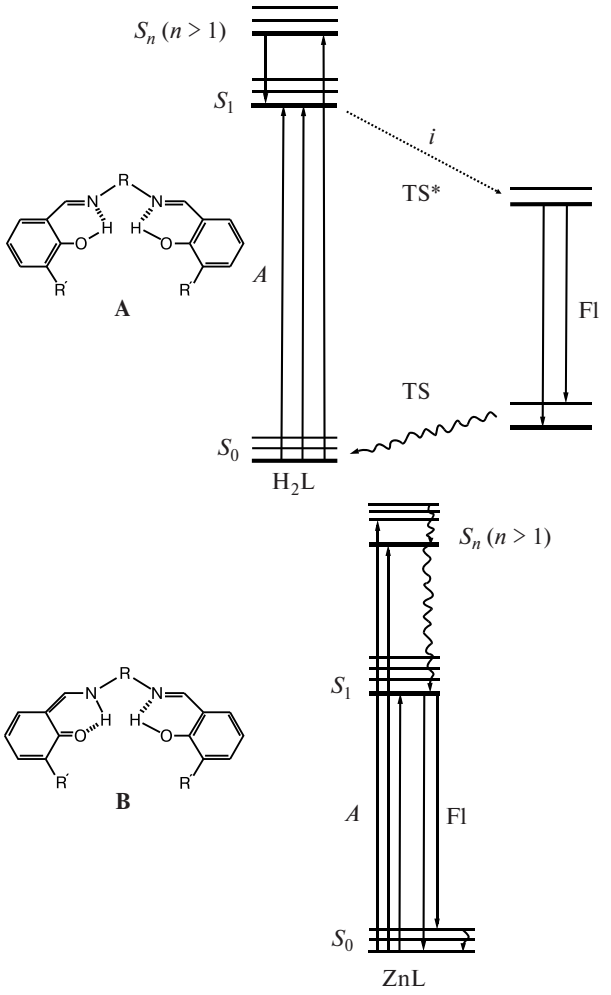

Fig. 8. Scheme of electronic transitions for photoluminescence of the Schiff bases and zinc(II) complexes[42,43]: *A* is absorption, Fl is fluorescence, TS is transition state, and *i* is intramolecular proton transfer in the excited molecule.

zinc(II) ion is a distorted square pyramid; however, this is due to coordination of the water molecules in the first case and to coordination of the oxygen atom of the neighboring molecule and dimer formation in the second case. The decrease in the gap width Δ(HOMO—LUMO) and the bathochromic shift of the emission maximum in the photoluminescence spectra are apparently caused by the formation of binuclear clusters in the case of $[Zn(SAL)^1]_2$ and, as a consequence, by the change in the MO structures and the nature of transitions. In particular, from the results of theoretical modeling of cluster compounds of d^{10}-metals with hydroxy/oxy bridges it follows that the HOMO is still the π-bonding orbital of the ligand, whereas the LUMO is the σ*-antibonding orbital, which is mainly due to the formation of the metal—oxygen bond and is localized on the metal center.[5,44] Thus, in the case of $[Zn(SAL)^1]_2$ one likely deals with the change in the nature of the energy transition, inducing the photoluminescence.

Here, the emission is due to the charge transfer from the ligand π-orbital to the 5s-orbital of the zinc(II) ion.

Analysis of the relative quantum yields and photoluminescence decay times (see Table 1) revealed no regular effect of the modification of organic ligands and complexation; only certain trends can be mentioned. For instance, the introduction of a methoxy group leads to a decrease in the relative quantum yields and the excited-state lifetimes of both H_2L and $ZnL \cdot H_2O$, whereas replacement of the ethylenediamine bridge by the *o*-phenylenediamine one causes φ_{rel} and τ_{obs} to increase for the Schiff bases, but to decrease for the zinc(II) complexes. Among the H_2L compounds studied, the highest relative quantum yield was observed for $H_2(SAL)^2$ derived from *o*-phenylenediamine and salicylaldehyde. A strong photoluminescence quenching and decrease in the photoluminescence decay time observed for the ethylenediamine and *o*-vanillin derivative ($H_2(MO)^1$) is probably due to the π—π-stacking in the structure of this compound.[45,46] The complexation with zinc(II) leads to the increase in φ_{rel} and τ_{obs} for the ethylenediamine derivatives $H_2(SAL)^1$ and $H_2(MO)^1$, whereas a decrease in these values is observed for the *o*-phenylenediamine derivatives $H_2(SAL)^2$ and $H_2(MO)^2$.

In conclusion, we have studied the effect of conjugation enhancement, introduction of electron-donating substituent, and complexation on the photoluminescent and thermal properties of tetradentate Schiff bases (H_2L), salicylaldehyde and *o*-vanillin derivatives $H_2(SAL)^1$, $H_2(SAL)^2$, $H_2(MO)^1$, and $H_2(MO)^2$, and the corresponding zinc(II) complexes. Peculiarities of the synthesis of the zinc(II) complexes with Schiff bases have been considered. Explanation of changes in the relative quantum yields and the luminescence decay times of the modified Schiff bases and complexes requires more detailed investigations involving recording of time resolved spectra, theoretical modeling of excited states of molecules, determination of the crystal structure of each compound, *etc*. Nevertheless, the results obtained in this study allow the zinc(II) complexes obtained to be recommended as EL materials for the design of OLED with allowance for their thermal stability and photoluminescent properties.

The authors are grateful to A. V. Mironov (M. V. Lomonosov Moscow State University) for the measurement of the X-ray patterns of powdered zinc(II) complexes.

This work was financially supported by the Russian Foundation for Basic Research (Project Nos 07-02-00495a, 09-02-00546a, and 09-03-00850a).

References

1. H. Tanaka, S. Tokito, Y. Taga, A. Okada, *J. Mater. Chem.*, 1998, **8**, 1999.
2. S. Wang, *Coord. Chem. Rev.*, 2001, **251**, 79.
3. R. C. Evans, P. Douglas, C. J. Winscom, *Coord. Chem. Rev.*, 2006, **250**, 2093.
4. A. V. Metelitsa, A. S. Burlov, S. O. Bezuglyi, I. G. Borodkina, V. A. Bren´, A. D. Garnovskii, V. I. Minkin, *Coordinats. Khim.*, 2006, **32**, 894 [*Russ. J. Coord. Chem.*, 2006, **32**, 858 (Engl. Transl.)].
5. S.-L. Zheng, X.-M. Chen, *Aust. J. Chem.*, 2004, **57**, 703.
6. S. Lamansky, P. Djurovich, D. Murphy, F. Abdel-Razzaq, H.-E. Lee, C. Adachi, P. E. Burrows, S. R. Forrest, M. E. Thompson, *J. Am. Chem. Soc.*, 2001, **123**, 4304.
7. Y. W. Shi, M.-M. Shi, J.-C. Huang, H.-Z. Chen, M. Wang, X.-D. Liu, Y.-G. Ma, H. Xu, B. Yang, *Chem. Commun.*, 2006, 1941.
8. C. Pérez-Bolivar, V. A. Montes, P. Anzenbacher, *Inorg. Chem.*, 2006, **45**, 9610.
9. R. Pohl, P. Anzenbacher, *Org. Lett.*, 2003, **5**, 2769.
10. S. Mizukami, H. Houjou, K. Sugaya, E. Koyama, H. Tokuhisa, T. Sasaki, M. Kanesato, *Chem. Mater.*, 2005, **17**, 50.
11. M. E. Germain, T. R. Vargo, P. G. Khalifah, M. J. Knapp, *Inorg. Chem.*, 2007, **46**, 4422.
12. W.-K. Lo, W.-K. Wong, W.-Y. Wong, J. Guo, K.-T. Yeung, Y.-K. Cheng, X. Yang, R. A. Jones, *Inorg. Chem.*, 2006, **45**, 9315.
13. V. Coropceanu, J. Cornil, D. A. da Silva Filho, Y. Olivier, R. Silbey, J.-L. Brédas, *Chem. Rev.*, 2007, **107**, 926; Y. Shirota, H. Kageyama, *Chem. Rev.*, 2007, **107**, 953.
14. P. G. Gozzi, L. S. Dolci, A. Garelli, M. Montalti, L. Prodi, N. Zaccheroni, *New. J. Chem.*, 2003, **27**, 692.
15. T. Sano, Y. Nishio, Y. Hamada, H. Takahash, T. Usuki, K. Shibata, *J. Mater. Chem.*, 2000, **10**, 157.
16. S. H. Hwang, P. Wang, C. N. Moorefield, J.-Che. Jung, J.-Y. Kim, S.-W. Lee, G. R. Newkome, *Macromol. Rapid Commun.*, 2006, **27**, 1809.
17. N. Yoshida, K. Ichikawa, M. Shiro, *J. Chem. Soc., Perkin Trans.*, 2000, **2**, 17.
18. W. Lu, M. C. W. Chen, K.-K. Cheung, Ch.-M. Che, *Organometallics*, 2001, **20**, 2477.
19. H. Schiff, *Ann. Suppl.*, 1864, **3**, 43.
20. M. J. O´Conner, B. O. West, *Aust. J. Chem.*, 1967, **20**, 2077.
21. G. E. Bately, D. P. Graddon, *Aust. J. Chem.*, 1967, **20**, 885.
22. C. de Mello Donegá, S. A. Junior, G. F. de Sa, *Chem. Commun.*, 1996, 1199.
23. C. Lee, W. Yang, R. G. Parr, *Phys. Rev. B*, 1988, **37**, 785.
24. P. J. Hay, W. R. Wadt, *J. Chem. Phys.*, 1985, **82**, 270.
25. V. Bertolasi, P. Gilli, V. Ferretti, G. Gilli, *J. Am. Chem. Soc.*, 1991, **113**, 4917.
26. P. Gilli, V. Bertolasi, V. Ferretti, G. Gilli, *J. Am. Chem. Soc.*, 2000, **122**, 1045.
27. D. Hall, F. H. Moore, *J. Chem. Soc. (A)*, 1966, 1822.
28. M. Odoko, N. Tsuchida, N. Okabe, *Acta Crystallogr.*, 2006, **E62**, m708.
29. A. de Bettencourt-Dias, *Dalton Trans.*, 2007, 2229.
30. W.-Y. Wong, G.-L. Lu, L. Liu, J.-X. Shi, J. Lin, *Eur. J. Inorg. Chem.*, 2004, 2066.
31. S.-L. Zheng, J.-P. Zhang, X.-M. Chen, Z.-L. Huang, Z.-Y. Lin, W.-T. Wong, *Chem. Eur. J.*, 2003, **9**, 3888.
32. T. Sekikawa, T. Kobayashi, T. Inabe, *J. Phys. Chem. B*, 1997, **101**, 10645.
33. H. Joshi, F. S. Kamounah, C. Gooijer, G. Van der Zwan, L. Antonor, *J. Photochem. Photobiol. A: Chem.*, 2002, **152**, 183.
34. M. Ziółek, J. Kubicki, A. Maciejewski, R. Nasręcki, A. Grabowska, *Chem. Phys. Lett.*, 2003, **369**, 80.

35. K. Amimoto, T. Kawato, *J. Photochem. Photobiol. C: Photochem. Rev.*, 2005, **6**, 207.
36. D. LeGourriérec, V. A. Kharlanov, R. G. Brown, W. Rettig, *J. Photochem. Photobiol. A: Chem.*, 2000, **130**, 101.
37. K. Ueno, A. E. Martell, *J. Phys. Chem.*, 1956, **60**, 1270.
38. A. Filarowski, *J. Phys. Org. Chem.*, 2005, **18**, 686.
39. F. Liang, J. Chen, Y. Cheng, L. Wang, D. Ma, X. Jing, F. Wang, *J. Mater. Chem.*, 2003, **13**, 1392.
40. S.-M. Yue, H.-B. Xu, J.-F. Ma, Z.-M. Su, Y.-H. Kan, H.-J. Zhang, *Polyhedron*, 2006, **25**, 635.
41. Y.-P. Tong, S.-L. Zheng, X.-M. Chen, *J. Mol. Struct.*, 2007, **826**, 104.
42. Y.-P. Tong, S.-L. Zheng, X.-M. Chen, *Inorg. Chem.*, 2005, **44**, 4270.
43. Y.-P. Tong, S.-L. Zheng, X.-M. Chen, *Eur. J. Inorg. Chem.*, 2005, 3734.
44. S.-L. Zheng, J.-H. Yang, X.-L. Yu, X.-M. Chen, W.-T. Wong, *Inorg. Chem.*, 2004, **43**, 830.
45. D. Cunningham, K. Giligan, M. Hannon, C. Kelly, P. McArdle, A. O´Malley, *Organometallics*, 2004, **23**, 984.
46. M. E. Germain, T. R. Vargo, P. G. Khalifah, M. J. Knapp, *Inorg. Chem.*, 2007, **46**, 4422.

Received September 11, 2007;
in revised form April 28, 2008